Laser generated tool surface out of metal matrix composite

Freiße, H.*[1], Hohenäcker, V.[1], Seefeld, T.[1], Vollertsen, F.[1,2]

[1]BIAS – Bremer Institut für angewandte Strahltechnik GmbH, Klagenfurter Straße 5, D-28359 Bremen, Germany
[2]University of Bremen, Bibliothekstr. 1, D-28359 Bremen, Germany

Abstract

Avoiding lubricants in metal forming offers the possibility of ecological and environmental optimization of industrial production processes. There is a necessity for novel approaches of tool surfaces to withstand higher loads in Dry Metal Forming. In this work, the production technology of a laser generated tool surface with a supporting plateau out of hard particles and its behavior in tribological interaction with high alloy steel are presented. The hard particles stand out of the tool surface and are in direct contact with the sheet material. The influence of the laser energy input on the ablation depth of the metallic matrix and on the ablation depth of the hard particles was investigated. Strip drawing test was applied to determine the friction coefficient as a function of the depression.

Keywords: functional layers, metal matrix composite (MMC), laser melt injection, laser ablation, Dry Metal Forming

1 Introduction

Deep drawing without lubricants leads to high loads to the tool surface [1]. According to the current state of the art, dry deep drawing is not industrially applicable. New tool surface concepts have to be developed and evaluated to ensure process reliability in dry metal forming.

An approach is to modify the chemical composition of the tool material. The wear resistance in dry sliding could be increased significantly by reinforcing for example aluminum with 4% tungsten carbid particles and 6% red mud [2], aluminum with 10% aluminum oxide particles [3] or bronze with Ni3Al particles [4].

Another approach is to modify the geometry of the tool surface. Different dimensions of the surface structures were applied. Investigations are presented by integrating macro structures in the blank holder area of a deep drawing tool to reduce the friction coefficient by controlling the material flow [5]. The macro structure showed a waviness shape. To receive an appropriate dry forming process a depression of 0.2 mm and a structure period of 8 mm was investigated to induce an alternating bending mechanism in the sheet material. Influencing the tribological system in dry forming by structured tools were also tested for bulk forming processes, for e.g. in rotary swaging [6]. The structure had a cosine geometry with a depression up to 0.2 mm and a structure period up to 1.3 mm. Laser textured tetrahedral amorphous carbon (ta-C) coatings lead to 20% lower

friction coefficients in strip drawing test against steel DC04 [7]. The micro features in the tool surface had a width of 500 µm und a length of 200 µm. The depth amounted from 0.5 µm to 5 µm and the contact ratio was reduced up to 50% by laser ablation. The positive mechanisms of the micro features depended on the contact ratio. Micro-structuring of ta-C coatings with a depression of 0.25 µm and a structure period of 10 µm were produced by deploying Direct Laser Interference Patterning technology [8]. Using these structured surfaces reduced the tool wear in dry sliding.

In this work the production technology is presented to manufacture functional layers with hard particles standing out of the surface forming a supporting plateau which is in direct contact with the sheet material. The influence of the depression on the friction coefficient was investigated.

2 Experimental details

2.1 Laser melt injection

The materials, equipment and the process parameters of the laser melt injection process are listed in Tab. 1.

Tab. 1. Materials, equipment and the process parameters of the laser melt injection process

Laser	Trumpf HL4006D	Substrate	CuAl10Ni5Fe4
Wavelength	1064 nm	Dimensions	10 x 21 x 30 mm³
Fiber diameter	600 µm	Particles	SFTC
Collimation length	200 mm	Particle size	-106+45 µm
Focusing length	200 mm	Powder feeding rate	25 g/min
Spot diameter	6 mm	Feeding gas	Argon
Laser power	3 kW	Feeding gas flow rate	8 l/min
Shielding gas	Argon	Process head	Precitec YC50
Centric flow rate	16 l/min	Travel speed	300 mm/min
Coaxial flow rate	8 l/min	Overlapping degree	40 %

The overlapping degree of the laser melt injected tracks OD_T was calculated by the equation (Eq. 1) under consideration of the track width w and the track offset Δy.

$$OD_T = (w - \Delta y) / w \cdot 100 \% \qquad (1)$$

The required geometry of the strip drawing jaws was manufactured by wire eroding using the eroding machine AGIE Evolution 2 and a wire diameter of 0.3 mm.

2.2 Laser ablation

Tab. 2 is showing the equipment and the process parameters of the laser ablation process.

Tab. 2: Equipment and process parameters for laser ablation

Laser	Trumpf TruMiro5050	Repetition rate	200 kHz
Wavelength converter Xiton Box		Pulse duration	< 10 ps
Converted wavelength	515 nm	Scanner Scanlab hurryscan II 14	
Focusing length	196 mm	Scanning speed	< 15 m/s
Focus diameter	29.4 µm	Scan field	120 x 120 mm²
Pulse energy	> 5 µJ < 150 µJ	Linear axis	ISEL LES 5
Average power	30 W	Position accuracy	± 0.02 mm

The Rayleigh length z_R was calculated by equation (2) under consideration of the focus radius ω_f, the wavelength λ and the diffraction index M^2.

$$z_R = \pi \cdot \omega_f^2 / (\lambda \cdot M^2) \qquad (2)$$

Equation (3) was used to determine the laser spot diameter d_{LS} analytically depending on the defocusing length z.

$$d_{LS} = 2 \cdot (1 + (z/z_R)^2)^{0.5}$$

The overlapping degree OD_P of the laser pulses was calculated by the equation (4) under consideration of the scanning speed v_S, the repetition rate f_{rep} and the spot diameter d_{LS}.

$$OD_P = (1 - v_S)/(f_{rep} \cdot d_{LS}) \cdot 100 \% \qquad (4)$$

2.3 Tribological testing

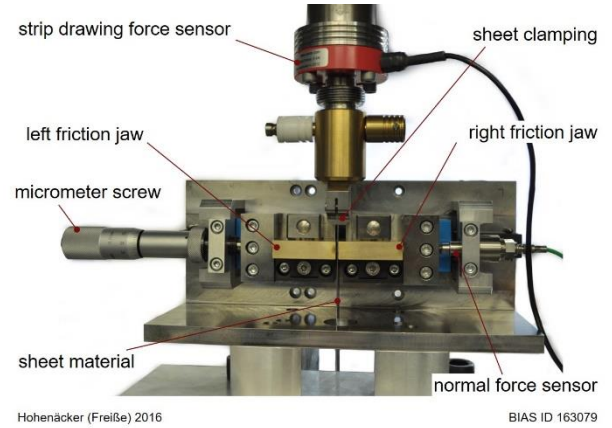The strip drawing apparatus is shown in Figure 1.

Figure 1: Strip drawing apparatus

The strip drawing apparatus was installed in a compression-tension machine Zwick Roell Z250. The strip drawing force sensor had max. testing load of 5 kN and a measurement uncertainty of ± 10 N. The normal force sensor Kistler 9217A had a max. testing load of 500 N and a measurement uncertainty of ± 1% of the current measuring value.

The sheet material was out of 1.4301 and had a thickness of 0.5 mm. The roughness amounted to Sa = 0.22 µm. The dimensions of the strip drawing sheets were 140 x 11.4 mm². The contact pressure during strip drawing was adjusted to 2.5 MPa.

The strip drawing length was 90 mm. The friction coefficient was calculated as an average value in the evaluation range between the 45 mm to 85 mm to ensure a constant speed of 10 mm/s, see Fig. 2.
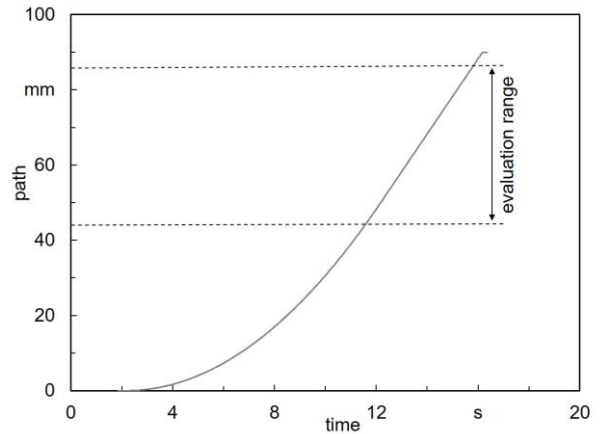
Figure 2: Path-time motion of the compression-tension machine

2.4 Topography measurement

The topography of the laser generated surface was measured by using the 3D laser scanning confocal microscope Keyence VK-9700.

The roughness measurement was carried out according to ISO 25178 using an objective with 50x optical zoom and a measurement field of 200 x 200 µm². The low-pass filter (S-filter) was 0.8 µm and the high-pass filter (L-filter) amounted to 0.2 µm.

The ablation depth was measured by using an objective with 20x optical zoom with a measuring field of 708 x 531 µm². Three linear profile sections were ap-

plied in horizontal and vertical direction. So the average value and standard deviations was calculated from six measurements.

3 Results

3.1 Laser melt injection

The width of the laser melt injected tracks amounted to 3.6 mm. To achieve an overlapping degree of 40% a track offset of 2.16 mm was chosen. So the cladding amounted to 648 mm²/min. Fig. 3 is showing the laser generated MMC surface on a strip drawing jaw.
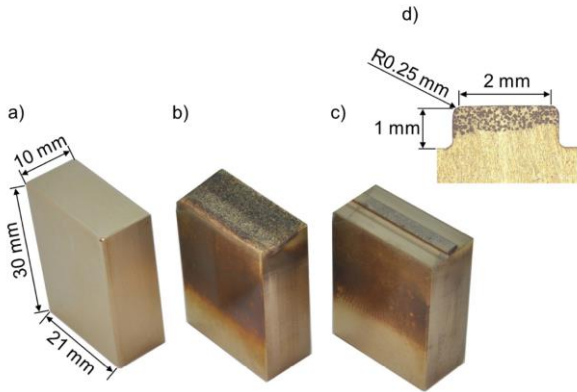

Figure 3: Laser generated MMC surface on a strip drawing jaw.
a) dimensions of the strip drawing jaw substrate, b) laser melt injected tracks, c) finished eroded shape shown in overview and d) in metallographic cross section

3.2 Laser ablation

Figure 4 is showing the influence of the focus position on the diameter of the ablation field using a substrate material without hard particles. Applying higher pulse energy leads to greater ablation diameters. Increasing the laser power of 500% resulted in an increase of 20% of the ablation diameter in focus position and 54% in defocused position of 4 mm.
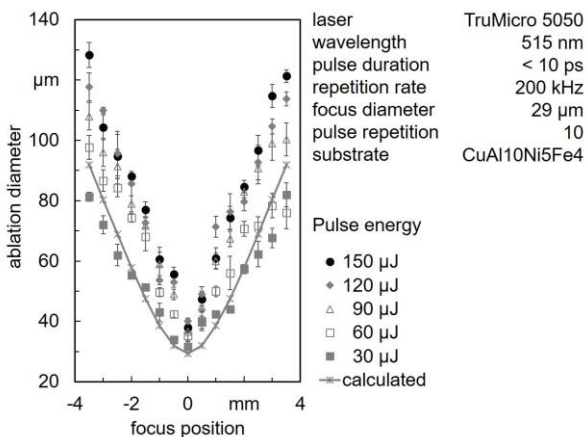

Figure 4: Ablation diameter as a function of the focus position

The ablation depth of the matrix referring to the initial state of the surface h_M and the depression h_{PV} as a function of the laser spot diameter and the pulse energy is given in Fig. 5. Increasing the laser spot diameter leads to a decreased ablation depth. Applying a higher pulse energy of 33% resulted in a higher ablation depth

of the matrix referring to the initial state of the surface h_M of 38% $\pm$ 10% and in an increased depression h_{PV} of 36% $\pm$ 16%.
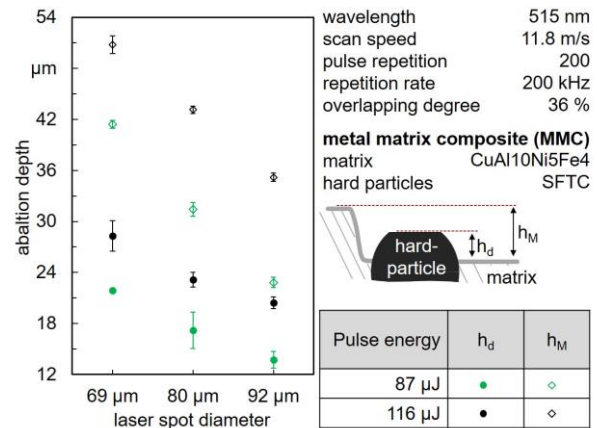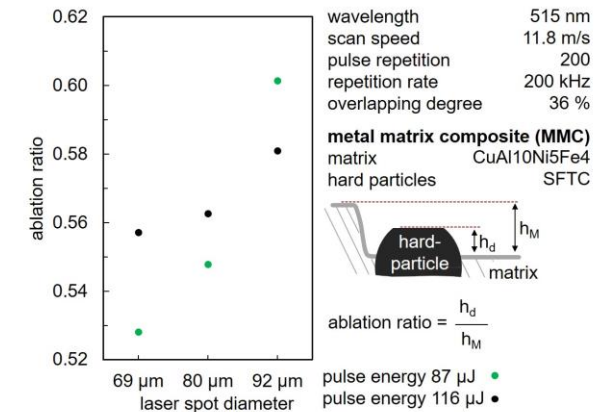

Figure 5: Influence of the laser spot diameter and pulse energy on the ablation depth of the hard particles and the matrix

The ratio of the depression h_{PV} and the total ablation depth h_M is defined as the ablation ratio q_{AR}. In Fig. 6 it can be seen, that increasing the laser spot diameter leads to a higher ablation ratio.
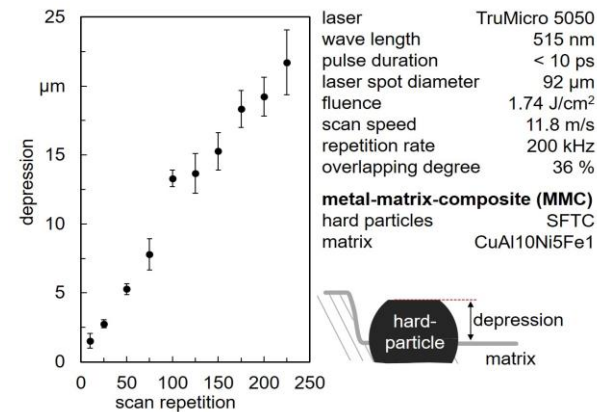

Figure 6: Influence of the pulse energy and laser spot diameter on the ablation quotient

By higher pulse repetition of the laser ablation process an increase of the depression can be achieved (Fig. 7).

Figure 7: Depression as a function of the pulse repetition

Figure 8 is showing a top view of the laser generated MMC tool surface with a depression of 20 µm. The top view figure and the profile section are illustrating the supporting plateau out of hard particles which is in direct contact with the sheet material.
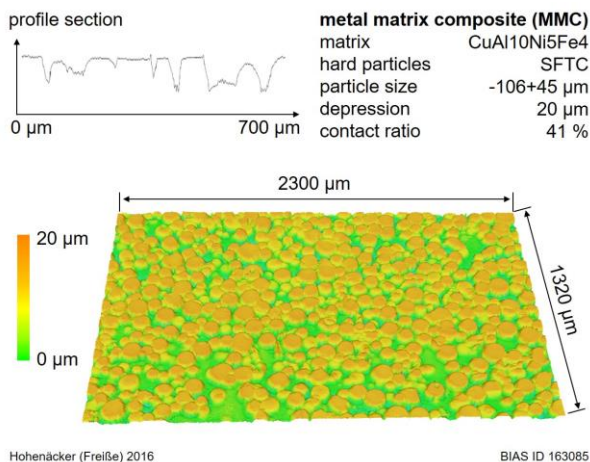

Figure 8: Top view of the laser generate MMC tool surface

3.3 Tribological testing

The friction coefficient as a function of the depression in dry and lubricated strip drawing is shown in Fig. 9.
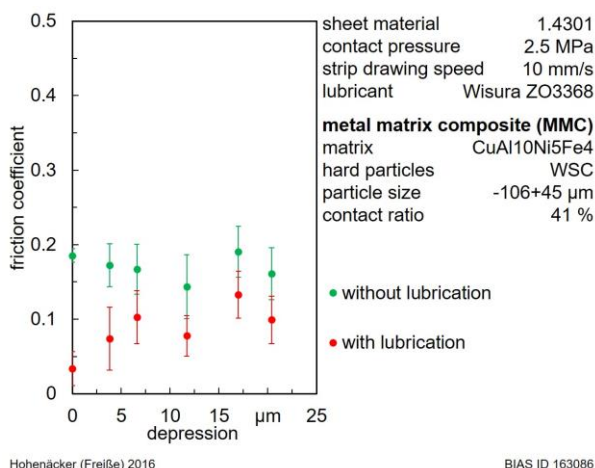

Figure 9: Friction coefficient depending on the depression

In the tribological system without lubrication an average of the friction coefficient of 0.17 ± 0.02 was investigated. Using lubricant and a higher depression resulted in a slight increase of the friction coefficient.

4 Discussion

The target of the laser ablation process is to receive a defined depression of the MMC tool surface. So there is the necessity to ablate the matrix of the composite material and it is undesirable to ablate the particles. The laser ablation ratio is an evaluation criterion for the efficiency of the laser ablation process. An ablation ratio of 1 means that there is no ablation of the hard particles. Using lower fluence in the laser ablation process improves the efficiency of the laser ablation process.

Deploying an MMC tool surface with a supporting plateau out of hard particles with a spherical form there

is a significant influence of the depression on the friction coefficient [9]. Using a supporting plateau with eroded particles as presented in this work, there is no influence of the depression on the friction coefficient. An increase of the depression up to 20 µm without an increase of the friction coefficient is an indication that the sheet is only in contact with the supporting plateau out of the hard particles or there is no contact between the sheet and the copper matrix of the MMC material.

5 Conclusion

Wear of the hard particles would lead to a change of the depression in the MMC surface during the industrial forming process. However, within this work it was shown that there is no significant influence of depression on the friction coefficient. So it can be concluded the laser generated tool surface can ensure reliability processes in dry metal forming.

References

[1] F. Vollertsen, F. Schmidt: Dry Metal Forming: Definition, chances and challenges. Int. J. Precision Engineering and Manufacturing – Green Technology 1/1 (2014) 76-77

[2] N.D. Chinta, N. Selvaraj, M. Mahesh: Dry sliding wear behaviour of aluminum red mud tungsten carbide hybrid metal matrix composites. IOP Conf. Series: Materials Science and Engineering 149 (2016) 1-7

[3] A. Pramanik: Effects of reinforcement on wear resistance of aluminum matrix composites. Trans. Nonferrous Met. Soc. China 26 (2016) 348−358

[4] I. Celikyürek, A. Bicer: Dry sliding friction and wear behavior of bronze matrix composites reinforced with Ni3Al particles: Comparison with conventional brake lining. Int. J. Mater. Res. (formerly Z. Metallkd.) 107 (2016) 835-841

[5] A. Brosius, A. Mousavi: Dry Metal Forming: Lubricant free deep drawing process by macro structured tools. CIRP Annals – Manufacturing Technology 65 (2016) 253-256

[6] M. Herrmann, C. Schenck: Dry Rotary Swaging with Structured Tools. Procedia CIRP 40 (2016) 653-658

[7] M. Merklein, M. Schmidt, S. Tremmel, K. Andreas, T. Häfner, R. Zhao, J. Steiner Tailored modifications of amorphous carbon based coatings for dry deep drawing. Dry Met. Forming OAJ FMT 2 (2016) 025–039

[8] T. Kunze, A. Mousavi, Th. Stucky, F. Böttcher, T. Roch, A. Brosius, A. Lasagni: Tribological Optimization of Dry Forming Tools. Dry Met. Forming OAJ FMT 2 (2016) 078-082

[9] H. Freiße, A. Langebeck, H. Köhler, T. Seefeld: Dry strip drawing test on tool surfaces reinforced by hard particles. Dry Met. Forming OAJ FMT 2 (2016) 001–006